

Development of Wear-Resistant Coatings for Cobalt-base Alloys

B.V. Cockeram

USDOE contract No. DE-AC11-98PN38206

RECEIVED
NOV 02 1999
STI

NOTICE

This report was prepared as an account of work sponsored by the United States Government. Neither the United States, nor the United States Department of Energy, nor the United States Navy, nor any of their employees, nor any of their contractors, subcontractors, or their employees, makes any warranty, express or implied, or assumes any legal liability or responsibility for the accuracy, completeness or usefulness of any information, apparatus, product or process disclosed, or represents that its use would not infringe privately owned rights.

BETTIS ATOMIC POWER LABORATORY

WEST MIFFLIN, PENNSYLVANIA 15122-0079

Operated for the U.S. Department of Energy
by Bechtel Bettis, Inc.

DISCLAIMER

Portions of this document may be illegible
in electronic Image products. Images are
produced from the best available original
document

Development of Wear-Resistant Coatings for Cobalt-base Alloys

B.V. Cockeram, Bettis Atomic Power Laboratory, Bechtel Bettis, Inc., P.O. Box 79, West Mifflin, PA 15122-0079.

Abstract

The level of nuclear plant radiation exposure due to activated cobalt wear debris could potentially be reduced by covering the cobalt-base materials with a wear resistant coating. Since most wear resistant coatings have a higher stiffness and hardness than cobalt-base alloys, support of the coating by the base material is a concern in high stress wear contact. Four approaches have been taken to minimize the differences in stiffness between the substrate and wear resistant coating: (1) the use of a thin Cr-nitride coating with a less-stiff interlayer, (2) the use of a thick, multilayered coating (Cr-nitride or Zr-nitride) with graded layers, (3) use of a duplex approach, or nitriding to harden the material subsurface followed by application of a multilayered Cr-nitride coating, and (4) application of ion nitriding or carburizing alone. Characterization of these coatings is discussed. The adhesion of the coatings is evaluated by scratch testing. Laboratory pin-on-disc and rolling contact wear tests were used to evaluate the wear performance of the coatings. Based on the results of laboratory wear tests, multilayer Cr-nitride coatings and ion nitriding are the most promising approaches.

Introduction

Although cobalt-base alloys have excellent wear resistance, the nuclear activation of cobalt wear debris to Co^{60} results in high radiation levels in nuclear plant applications [1,2]. The costs and risks resulting from nuclear plant contamination with Co^{60} debris could be reduced by using a low cobalt alloy or coating the currently used cobalt-base alloy with a wear-resistant coating [3]. Since the unique combination of wear and mechanical properties observed in cobalt-base alloys are rarely duplicated in cobalt-free systems, the use of a wear resistant coating may involve less risk. Potential failure of the wear resistant coating would only expose the wear resistant cobalt-base material.

Although cobalt-base alloys generally exhibit excellent wear resistance, these alloys are much softer than wear resistant coatings deposited by Physical Vapor Deposition (PVD). The use of a wear-resistant coating that has a higher stiffness and hardness than the base material is typically not viable in high stress wear applications [4,5]. High stress wear contact results in high interfacial stresses between a stiff coating and a softer substrate, which typically leads to catastrophic coating failure. Catastrophic coating failure produces large pieces of hard, abrasive coating debris that result in an increase in the wear rate of a system. Potential approaches for developing a wear-resistant coating that could be successfully used on a softer substrate in high stress wear contact include [4,5]: (1) use of a thicker coating, and (2) use of multilayer coatings with interlayers that are less stiff than the top coating layer and only slightly more stiff than the base alloy.

The approaches taken to develop coatings for cobalt-base alloys in this work are intended to produce an adherent coating through minimizing differences in hardness between the wear resistant coating and the base material [3]. The use of a thin, dual-layer chromium-nitride ($\text{Cr-N(ss)/Cr}_2\text{N}$) coating with a stiff outer layer (Cr_2N) and a less-stiff inner layer (Cr-N(ss)) is evaluated. Thick four-layer $\text{Cr-N(ss)/Cr}_2\text{N}$ and zirconium nitride coatings with less-stiff inner layers, and thick tungsten coatings were also developed. Duplex coating approaches that involve the use of ion nitriding to produce a hardened surface followed by application of a graded, dual-layer $\text{Cr-N(ss)/Cr}_2\text{N}$ coating are also used. Single-step ion nitriding or plasma carburizing processes are also evaluated to produce a thick hardened layer at the substrate surface. Since wear-resistant coatings are rarely applied to cobalt-base alloys, the development of these coatings is briefly described. Table 1 is a summary of these coating approaches. The coatings have been evaluated by scratch adhesion testing, nano-scratch testing and nano-indentation testing. A pin-on-disc and 4-ball wear test were used for wear testing. The most viable coating approaches are described.

Materials and Procedures

The nominal composition of two different cobalt-base alloys used in this work (Haynes 25 and Stellite 3) and iron-base alloy (17-4 PH) are given in Table 2. Haynes 25 was used to produce flats for scratch adhesion and nano-indentation testing (3.175 cm x 1.27 cm x 0.64 cm), discs for pin-on-disc wear testing (5.72 cm diameter X 0.76 cm thick),

Table 1. Summary of coating/surface modifications. Scratch adhesion critical load values, critical load values from nano-indentation testing, and hardness values are also given for coatings/surface modifications applied to Haynes 25 flats.

Coating/ Surface-Modification, Vendor	Average Thickness ± Standard Deviation [μm]	Hardness Number for Coating [VHN or KHN]	Scratch Adhesion Critical Load Value [kg]	Nano-indentation Test Results	
				Critical Load Value [mN]	Hardness / Modulus [GPa/GPa]
Uncoated Haynes 25	N/A	200-400 KHN	Not Measured	N/A	7.4 / 258.5
Candidates Only Subjected to scratch adhesion testing					
Four-layer Cr-N(ss)/Cr ₂ N Coating, ACT	10.4 ± 1.1	1930 VHN	7.5	NF	14.2 / 270.4
TiN Coating, GM	2-3	2500-3000 VHN	2.0 – 3.0	15	25.7 / 400.5
ZrN Coating, PST	8.9 ± 0.9	2150 VHN	5.1	15 – 17	26.0 / 405.9
Plasma Carburizing, SC	13.8 ± 4.2	N/A	Not Measured	8 – 10	N/A
Low-pressure Duplex Coating, ACT	0.6 ± 0.2 Diff. Zone = 1.1 ± 0.3	1670 VHN	7.0 – 8.0	23	14.2 / 258.5
Thick Duplex Coating, AHT + ACT	Cr-N(ss)/Cr ₂ N = 5.8 ± 0.6 Nitride Layer = 11.7 ± 1.3	1990 VHN	4.5 – 5.5	NF	5.8 / 183.1
Candidates Used for 4-ball Wear Testing					
Dual-layer Cr-N(ss)/Cr ₂ N Coating, ACT	0.9 ± 0.2	1930 VHN	5.0 – 7.0	22.0	19.3 / 290.5
Ion Nitriding, AHT	11.7 ± 1.3	700-1100 KHN	Not Measured	NF	1.4 / 66.7
Thin Duplex Coating, AHT + ACT	Cr-N(ss)/Cr ₂ N = 3.0 ± 1.2 Nitride Layer = 11.7 ± 1.3	1970 VHN	5.0 – 5.5	NF	Not Measured
Candidates Used for Pin-on-Disc Testing					
Dual-layer Cr-N(ss)/Cr ₂ N Coating, ACT	2.5	1910 VHN	3.5	Not Measured	Not Measured
Tungsten Coating, ACT	9.0	1600 VHN	Not Measured	Not Measured	Not Measured

- Notes:
1. ACT = Advanced Coating Technology Group, Materials Technology Laboratory, Northwestern University, Evanston, IL.
 2. AHT Corp. = Advanced Heat Treat Corporation, Waterloo, IA.
 3. PST = Praxair Surface Technologies, Inc., Indianapolis, IN.
 4. SC = Surface Combustion Corporation, Maume, OH.
 5. GM = General Magnaplate, Linden, NJ.
 6. NF = No Coating Failure Observed.
 7. N/A = Could Not Be Determined.

and drive ball (1.27 cm diameter, Grade 10) and cup (4.57 cm outer diameter, 2.15 cm inner diameter, 1.71 cm thick with a 0.66 cm radius for the raceway) components for 4-ball wear testing. Pins (1.3 cm length X 0.63 cm diameter with a 0.47 cm radius on the tip) for pin-on-disc testing and balls (1.27 cm diameter) for 4-ball wear testing were produced from Stellite 3. Separators (4.28 cm diameter X 0.70 cm thick with three equally spaced holes 1.31 cm in diameter) made from 17-4 PH were used in the 4-ball wear test.

The 4-ball wear tests were done at Falex Corporation, Sugar Grove, IL, and more details on the test have been reported [3,6]. Six test pieces are used in the 4-ball wear test: (1) Haynes 25 drive ball, (2) three Stellite 3 intermediate balls, (3) a 17-4 PH separator, and (4) a Haynes 25 cup. The Stellite 3 intermediate balls are placed in the separator and roll in contact within the radius of the Haynes 25 cup. The Haynes 25

drive ball is in ball-on-ball contact with the three intermediate balls. The drive ball is rotated at 1200 RPM for 20 hours to result in 300 RPMs for the intermediate balls. A 6.21 kg load applied to the drive ball, and the 30° contact angle from the separator results in 2.42 GPa Hertzian contact stresses on the ball surfaces [6]. The 4-ball wear test was performed in de-ionized water at room-temperature (20-30°C). The cup, drive ball, and intermediate balls were coated with three different candidates for the 4-ball wear test (Table 3): (1) thin, dual-layer Cr-N(ss)/Cr₂N coating, (2) an ion nitrided base material, and (3) thin duplex coating.

The pin-on-disc wear testing was performed at Advanced Coating Technology Group at Northwestern University (ACTG) to evaluate the general wear performance of coated surfaces. A 6.804 kg load was applied to the Stellite 3 pin, which produces an initial estimated

Table 2. Nominal compositions of materials used in scratch adhesion, 4-ball wear, and pin-on-disc wear testing [Compositions in Weight%]

Alloy / Substrate	Co	Cr	W	Ni	Mn	C	Fe	Si	S	P	Other	Hardness HRC
Haynes 25 Flats and Discs	Bal	20.7	14.6	10.1	1.42	0.12	2.7	0.22	<.002	0.008	---	47
Haynes 25 Cups	Bal	20.4	14.6	10.1	1.43	0.09	2.17	0.16	<.002	0.013	---	52
Haynes 25 Balls	Bal	20.1	15.2	10.1	1.43	0.10	0.9	0.1	.0002	0.01	---	46
Stellite 3 Balls	Bal	30.04	11.82	1.82	0.35	2.20	1.66	0.81	0.012	0.012	.21 Mo .05 Ti	53
17-4 PH Separator	--	16.5	--	3.4	0.5	0.04	Bal	0.5	0.01	0.01	3.4 Cu 0.3 Nb	36

Hertzian contact stress of 345 MPa with the Haynes 25 disc. The rotational sliding speed was 0.1 m/s with a maximum run time of 30 minutes. The testing was done in room-temperature distilled water with friction and torque measured during the test. If the friction and torque values became excessively high, then the test was terminated. Only two types of coatings were applied to either the pin or the disc surface: (1) thin (2.5 μm), dual-layer Cr-N(ss)/Cr₂N coating, and (2) 9 μm thick layer of tungsten.

Scratch adhesion testing was performed (Table 1) using a spherical indenter. The critical load from scratch testing was determined by examinations of coating damage from scratches performed at a constant load. Nano-scratch adhesion testing was performed at MTS-Nano Instruments, Knoxville, TN using a 130 μm diameter sapphire sphere indenter at loads from 0 to 500 milli-Newtons and a cube corner indenter (100 μm) at loads up to 30 milli-Newtons [7,8]. The load was increased during nano-scratch adhesion testing, and large changes in the coefficient of friction or penetration depth versus scratch distance were used to identify the critical load. The hardness of the coatings was determined using a Vickers hardness indentation with a 10g load. A sharp Berkovich diamond indenter was used for nano-indentation testing in the continuous stiffness mode with at least seven indentations preformed [8]. The average hardness and average modulus versus depth were measured at a maximum indentation depth of 1-3 μm . The hardness versus depth profiles typically exhibited a peak with no apparent plateau, which indicates that substrate deformation was contributing to the measurement [8]. The nano-indentation modulus or hardness were determined at an indentation depth less than 1/10 of the coating thickness, see Table 1.

Results and Discussion

A. Coating Characterization and Scratch Testing

A1. Plasma Carburizing

One attempt was made to plasma carburize Haynes 25 using a glow discharge method in a methane atmosphere. The applied power density of 0.27 Watts/cm² produced a nominal substrate temperature of 593°C for the 48 hour run. A thick, porous deposit that primarily consisted of amorphous carbon and oxygen was produced by the plasma carburizing method [3]. The deposit produced by plasma carburizing exhibit poor adherence, and a low nano-scratch adhesion value was measured in Table 1. The porous deposit was so fragile that a hardness value could not be obtained. The hardness and adhesion testing indicate that these plasma carburizing conditions are not suitable for Haynes 25.

A2. Multilayer Zr-nitride, Cr-nitride, and tungsten coatings

A dual-layer zirconium-nitride (ZrN) coating was produced by a cathodic arc PVD process with a thick ($\approx 7.5 \mu\text{m}$) outer layer and a thin ($\approx 1.5 \mu\text{m}$) inner layer, see Table 1 [3]. The ZrN coating was determined by microprobe analysis and XRD to have the expected ZrN structure (ICDD card # 02-0956), but slight XRD peak shifts indicate that the coating has a different nitrogen stoichiometry (4.60 Å for the coating versus 4.56 Å for the ZrN in ICDD card # 02-0956). Higher critical load values are expected for thicker PVD coatings [4,9]. However, the critical load values determined for the ZrN coating by conventional scratch testing and nano-indentation testing were comparable to values measured for the thinner TiN and Cr-N(ss)/Cr₂N coatings (Table 1). The hardness values for the ZrN and TiN coatings are more than a factor of three higher than Haynes 25, which indicates that the ZrN and TiN coatings have not been sufficiently graded in hardness. The significant hardness difference between Haynes 25 and the ZrN or TiN coatings indicates that wear under high stress loading would likely result in coating failure [4,5]. A closer match in coating/substrate hardness and higher adhesion values are necessary.

Multi-layer chromium-nitride (Cr-N(ss)/Cr₂N) coatings consisting of an outer of chromium-nitride (Cr₂N) layer and an inner layer of chromium-nitrogen solid solution (Cr-N(ss)) were produced by a reactive, unbalanced magnetron (UBM) sputtering process, see Table 1 [3]. A thin (1 μm) two-layer Cr-N(ss)/Cr₂N coating with a 2:1 ratio of Cr-N(ss) to Cr₂N was applied to Haynes 25 flats, balls, and cup, and Stellite 3 balls. A thicker (2.5 μm) dual-layer Cr-N(ss)/Cr₂N coating with a 3:2 ratio of Cr₂N:Cr-N(ss) was deposited on Haynes 25 disc coupons. A thick four-layer Cr-N(ss)/Cr₂N coating ($\approx 10 \mu\text{m}$) with a 4 μm inner layer of Cr-N(ss) / 1 μm layer of Cr₂N / 4 μm layer of Cr-N(ss) / 1 μm outer layer of Cr₂N was deposited on Haynes 25 flats. A dense plasma was produced during the coating process that ionizes a high density of the nitrogen and chromium for improved reactivity, adhesion, and coating quality. A double rotation method was employed by mounting the coated parts on a rotating table in a rotating spindle for the flats, rotating wire basket fixture for the balls, and axial rotating spindle for the cups and discs. The increase in surface roughness for the thin coating ($R_a = 55 \text{ \AA} \rightarrow 82 \text{ \AA}$) after coating was small, with a larger increase in roughness ($R_a = 55 \text{ \AA} \rightarrow 271 \text{ \AA}$) observed for the thick four-layer Cr-N(ss)/Cr₂N coating. The microprobe image and chromium-map in Figures 1a and 1b show that the thick four- Cr-N(ss)/Cr₂N coating consists of alternating layers of 4 μm of Cr-N(ss) that are chromium-rich and 1 μm thick layers of Cr₂N that contain slightly less chromium. The thin dual-layer Cr-N(ss)/Cr₂N coating is about 1 μm thick, but the layers are too thin to be clearly resolved in the chromium map in Figure 1d. The thin dual-layer Cr-N(ss)/Cr₂N coating deposited on the Haynes 25 and Stellite 3 balls was similar in appearance and uniform in thickness. XRD analysis indicated that all of the Cr-

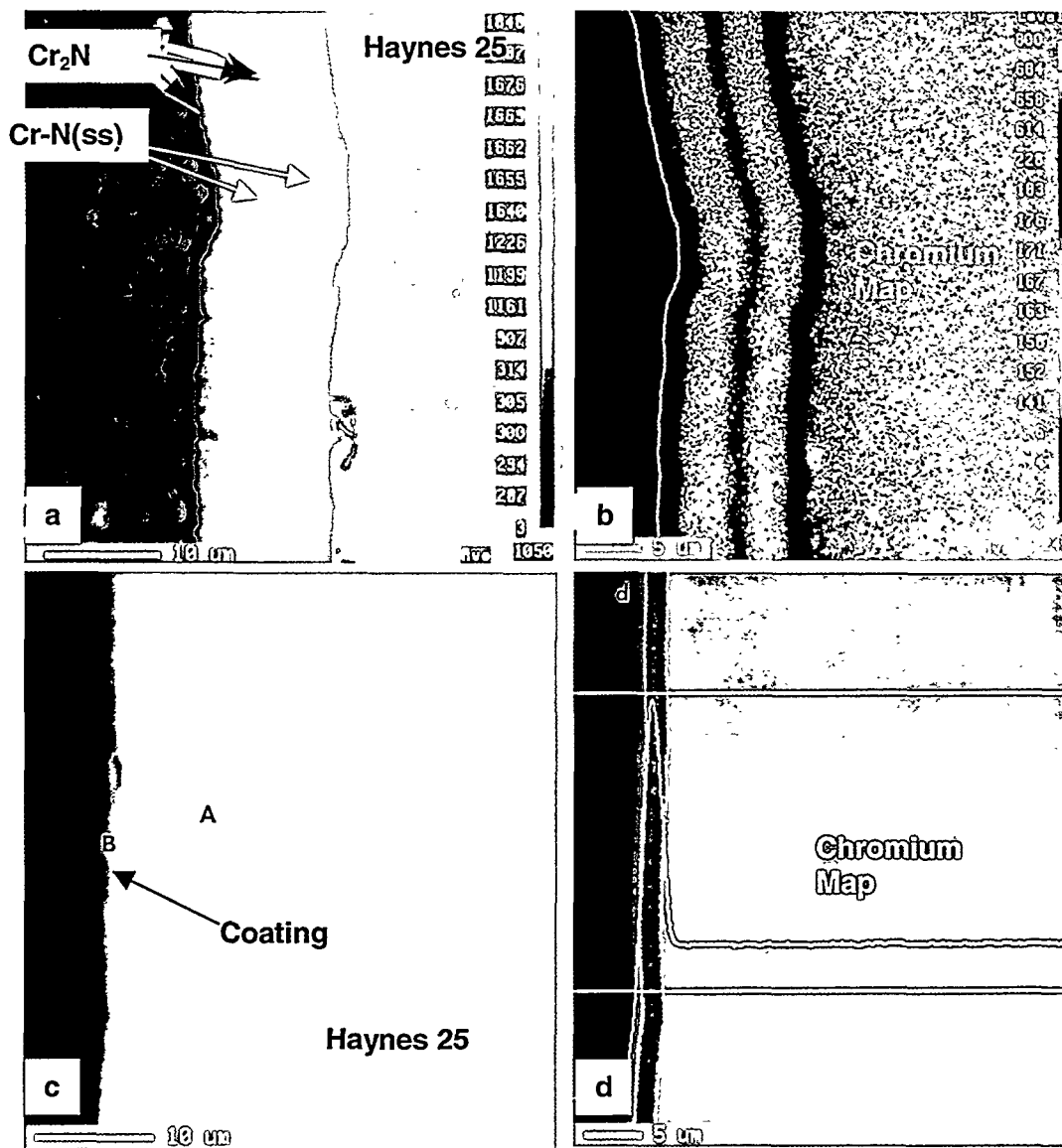


Figure 1. Microprobe analysis of Cr-N(ss)/Cr₂N coatings deposited on Haynes 25: (a) SEM/BSE image thick, four-layer Cr-N(ss)/Cr₂N coating, (b) X-ray map for chromium from region in Figure 1a, (c) SEM/BSE image of thin, dual-layer Cr-N(ss)/Cr₂N coating, (d) chromium map for Fig 1c.

N(ss)/Cr₂N coatings had layers of Cr₂N (ICCD Card #35-0803) and Cr-N(ss) as a chromium-nitrogen solid solution (Card #11-0065).

The scratch adhesion value for the thick four-layer Cr-N(ss)/Cr₂N coating was higher than that observed for the thinner Cr-N(ss)/Cr₂N coatings, which is generally expected for a thicker coating [9], see Table 1. Coating damage was not produced at the maximum applied load in the nano-scratch adhesion test (Table 1). The excellent adherence, and higher thickness of the four-layer Cr-N(ss)/Cr₂N coating probably results in no coating damage with the nano-indentation method. The Vickers hardness number (VHN) measured for the thick, four-layer Cr-N(ss)/Cr₂N coating in Table 1 was comparable to values measured for the thinner Cr-N(ss)/Cr₂N coatings. The hardness and modulus values measured using a nano-indentation method for the thick four-layer Cr-N(ss)/Cr₂N coating are close to the Haynes 25 base material. The nano-indentation depth was only 1 μm, which indicates that only the top two layers (1 μm outer layer of Cr₂N and 4 μm inner layer of Cr-N(ss)) of the four-layer coating were most affected in this test. The layered structure of the thick four-layer coating with a high fraction of a relatively compliant Cr-N(ss) layers (Figure 1a) likely results in nano-indentation hardness/modulus values that match the base

material. The composite layered structure of the thick four-layer Cr-N(ss)/Cr₂N coating apparently results in good damage resistance and adherence, and a match in nano-indentation hardness/modulus to the base material. These results indicate that the thick four-layered Cr-N(ss)/Cr₂N wear coating has promise for use under high stress loading.

The scratch and nano-indentation scratch values measured for the thin dual-layer Cr-N(ss)/Cr₂N coating were higher than values measured for the ZrN and TiN coatings. The scratch damage of the thin dual-layer Cr-N(ss)/Cr₂N coating produced in the adhesion tests was much more mild than the ZrN and TiN coatings, which indicates that the Cr-N(ss)/Cr₂N coatings were more adherent and damage resistant. The lower critical load value for the thicker 3:2 Cr-N(ss)/Cr₂N coating indicates that a higher fraction of Cr-N(ss) may be required for a thicker coating to exhibit good adhesion. The smaller coating thickness and lower fraction of more compliant Cr-N(ss) layer (Cr-N(ss):Cr₂N ratio of 2:1) in the thin dual-layer Cr-N(ss)/Cr₂N coating results in a slightly higher nano-indentation hardness and modulus value than the thick four-layer Cr-N(ss)/Cr₂N coating and the Haynes 25 base material. However, the hardness and modulus values for the thin dual-layer Cr-N(ss)/Cr₂N coating are a close match to the Haynes 25 substrate.

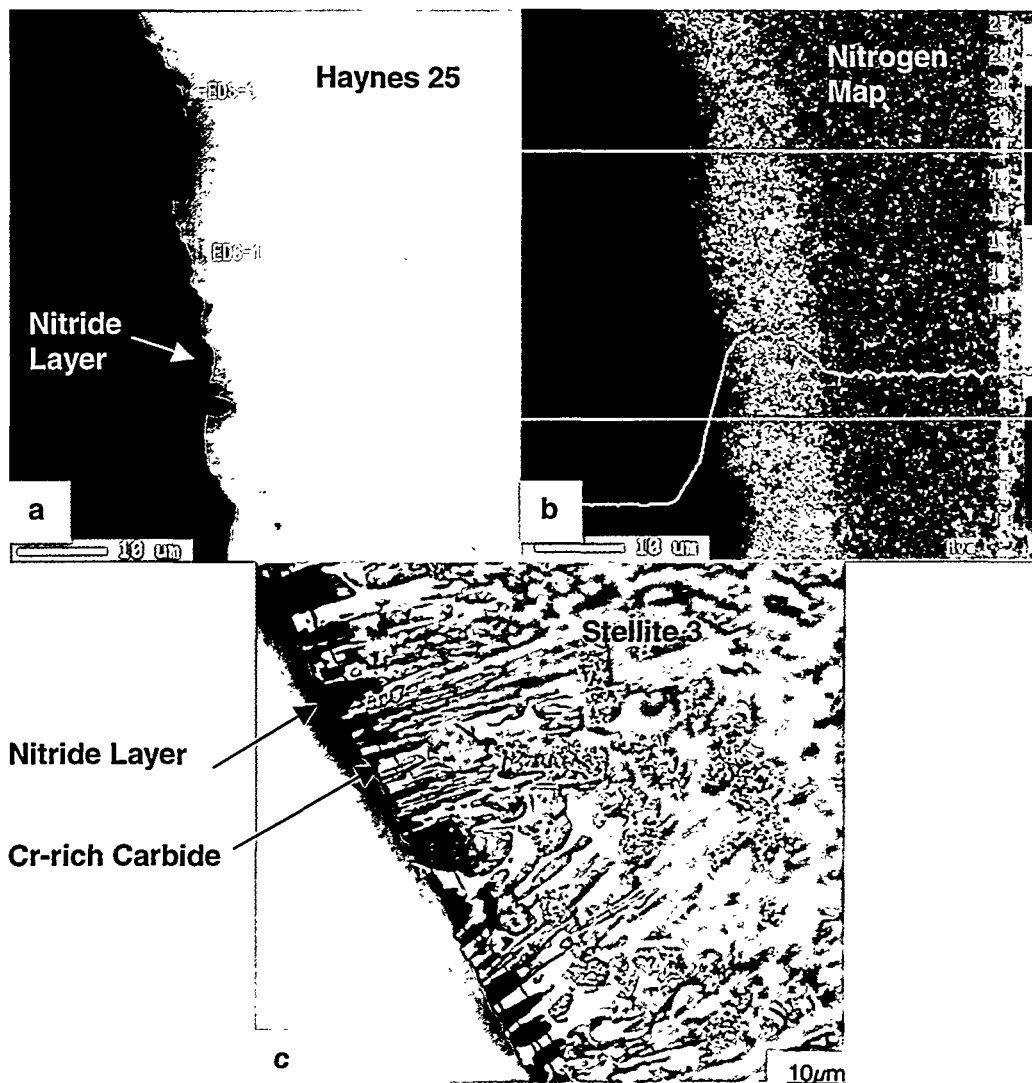


Figure 2. Cross-section of coupons after ion nitriding: (a) Haynes 25 flat, (b) nitrogen map of area in Fig. 2a with a line profile, (c) optical micrograph of Stellite 3 ball.

The tungsten coatings were produced by UBM deposition using a tungsten target in argon to produce a $9\ \mu\text{m}$ thick coating on Stellite 3 pins. SEM analysis indicated that the coating consisted of primarily tungsten, and the concentration of any trace elements was below the detection limit of EDS. The VHN number for the tungsten coating was slightly less than that observed for the Cr-N(ss)/Cr₂N coatings.

A3. Ion Nitriding

The commercial practice of ion nitriding involves the ionization of nitrogen gas in a dense plasma, and acceleration of the ionized nitrogen atoms into the substrate results in heating and diffusion of nitrogen into the surface for an increase in wear resistance and surface hardness [10]. Although ion nitriding has been used to improve the wear resistance of Stellite 6 [11], which is a cobalt-base alloy, information on the ion nitriding of Haynes 25 or Stellite 3 was not found. Three different ion nitriding treatments were initially tried (510°C for 48h, 566°C for 48h, and 566°C for 96h) [3]. The $556^\circ\text{C}/48\text{h}$ parameters resulted in a thick nitride layer with less thickness variation, and were used to produce the test coupons. A measurable increase in the surface roughness of the Haynes 25 balls ($R_a = 130\ \text{\AA} \rightarrow R_a = 2800\text{-}5300\ \text{\AA}$) and Haynes 25 cup ($R_a = 250\text{-}1300\ \text{\AA}$ to $R_a = 2800\text{-}4100\ \text{\AA}$) was produced by ion nitriding. The thermal activation and surface bombardment resulting from the ion nitriding process typically produces an increase in surface roughness

[10]. The influence of gas-phase or surface kinetics on the ion nitriding process may also result in a higher surface roughness [3].

An adherent and hard nitride layer with a diffusion zone that is about 1/4 the nitride layer thickness is formed by the ion nitriding of Haynes 25 [3], see Table 1 and Figure 2. The X-ray map for nitrogen shows in Figure 2b the high nitrogen content of the nitride layer, but the nitrogen content of the diffusion zone is below the WDS detection limit. An interference between the K-energy line for nitrogen and a L-energy line for cobalt results in the appearance of high nitrogen in the Haynes 25 substrate for the nitrogen map in Figure 2b. The true nitrogen content of the Haynes 25 substrate is below the detection limit ($<0.1\%$). The nitride layer is similar in composition to the base material and has the CrN structure (ICDD card # 11-0065) structure, i.e. this is a (Co,Cr,W,Ni,Fe)N nitride compound [3]. Stellite 3 consists of dendrites and interdendrite Cr-carbides, and ion nitriding results in the growth of a layer with a two-phase structure consisting of interdendritic Cr-carbide phases and a nitride ((Co,Cr,W,Ni,Fe)N) compound with the CrN (ICDD card # 11-0065) structure, see Figure 2c. A thin layer ($\approx 1\ \mu\text{m}$) rich in iron + carbon was observed on the outer surface of ion nitrided coupons. Deposition from the steel fixturing may have produced this iron-rich surface layer. Since the surfaces were fairly rough and covered with an iron-rich layer, it was difficult to obtain an

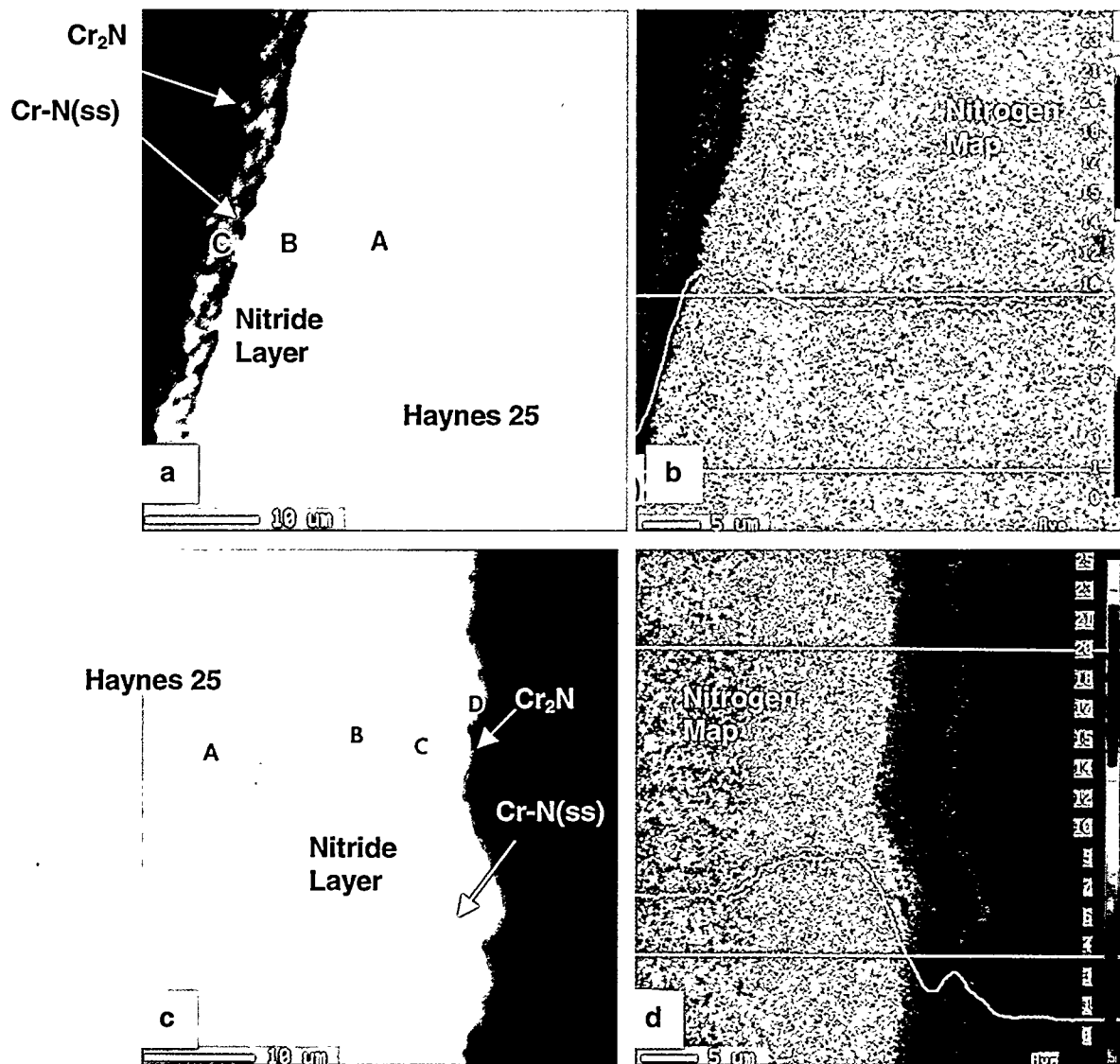


Figure 3. Microprobe analysis of duplex coatings deposited on Haynes 25: (a) thin duplex coating, (b) nitrogen map of Fig. 3a with a line profile, (c) thick duplex coating, and (d) nitrogen map of Fig. 3c with a nitrogen line profile.

accurate measurement of a nano-scratch adhesion value. A critical load was not detected at the maximum applied load using the nano-scratch test in Table 1. The nitride layer showed no evidence of spalling or cracking from the nano-scratch test. Some evidence of ductile smearing in the nano-scratch may result from the deformation of the 1 μm thick iron-rich layer on the surface of the nitride compound. The nano-indentation hardness/modulus values for the nitride layer were less than the Haynes 25 substrate. The depth of penetration of the nano-indenter is on the order of the thickness of the iron-rich surface layer (1 μm), which likely produces this low hardness value.

A4. Duplex Coatings (Ion Nitriding + Cr-N(ss)/Cr₂N Coatings)

Deposition of a Cr-N(ss)/Cr₂N coating on an ion nitrided surface is the duplex approach. An UBM process was used to produce two different Cr-N(ss)/Cr₂N coatings on ion nitrided substrates [3]: (1) a thin (1 μm) dual layer coating with a Cr-N(ss):Cr₂N ratio of 2:1, and (2) a thicker (6 μm) two-layer coating with a Cr-N(ss):Cr₂N ratio of 4:1. The rough surface of the ion nitride layer and surface iron-rich layer complicated the deposition of the coatings, but adherent deposits were produced. No change in surface roughness from ion nitriding to the duplex coated surface was observed for the Haynes 25 balls ($R_a = 2800\text{--}5300 \text{ \AA} \rightarrow R_a = 4100 \text{ \AA}$) and cup ($R_a = 2800\text{--}4100 \text{ \AA} \rightarrow R_a = 3300\text{--}4600 \text{ \AA}$). Low pressure ion nitriding in the sputter coating chamber at a

significantly lower total pressure, nitrogen pressure (6:1 ratio of nitrogen to argon) and shorter time (1 hour) followed by immediate application of a thin (0.7 μm) dual layer Cr₂N / Cr-N(ss) coating with a 3:2 ratio of Cr-N(ss):Cr₂N was also performed (low-pressure duplex coating). The increase in surface roughness for the substrates given the low-pressure duplex treatment was small ($R_a = 56 \text{ \AA} \rightarrow R_a = 173 \text{ \AA}$).

The thin duplex coating in Figure 3 consists of a nitride layer with an outer coating about 1 μm in thickness, see Table 1. The nitrogen X-ray map in Figure 3b shows the difference in the Cr₂N and Cr-N(ss) layers, the nitride layer and the Haynes 25 substrate. As observed for the ion nitrided coupons, the beam interference between the L-energy line for cobalt and the nitrogen line gives the appearance of high nitrogen in the Haynes 25 substrate. The thin duplex coating deposited on the Haynes 25 and Stellite 3 balls was also similar in appearance. Figures 3c and 3d show that the thick duplex coating consists of Cr-N(ss) and Cr₂N layers that are consistent with the 4:1 ratio for the 6 μm thick coating. A thin diffusion zone with an adherent Cr-N(ss)/Cr₂N outer coating was produced by the low-pressure duplex treatment, see Table 1. XRD analysis was used to confirm the presence of Cr₂N (ICDD card # 35-0803), chromium-nitrogen (Cr-N(ss)), and nitride layer for all the duplex coatings.

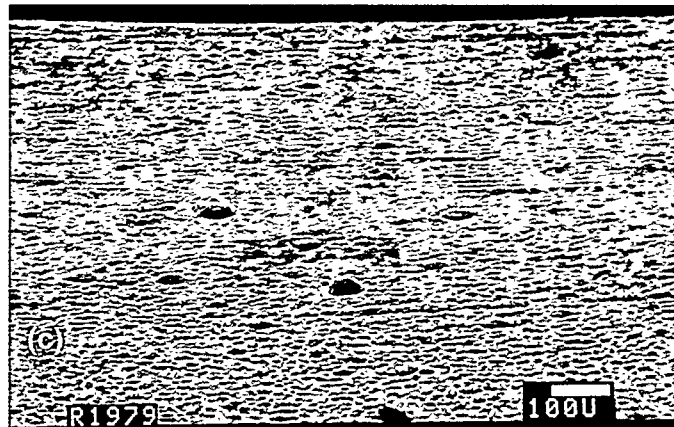
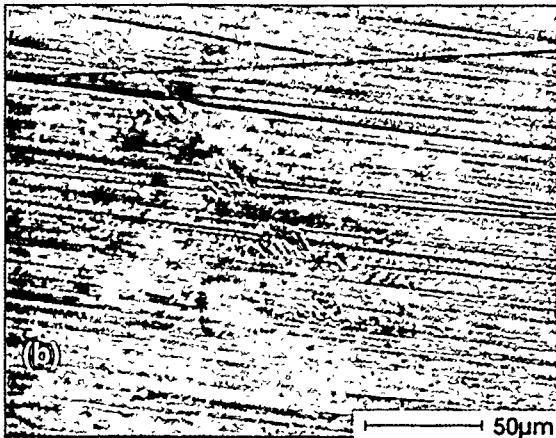
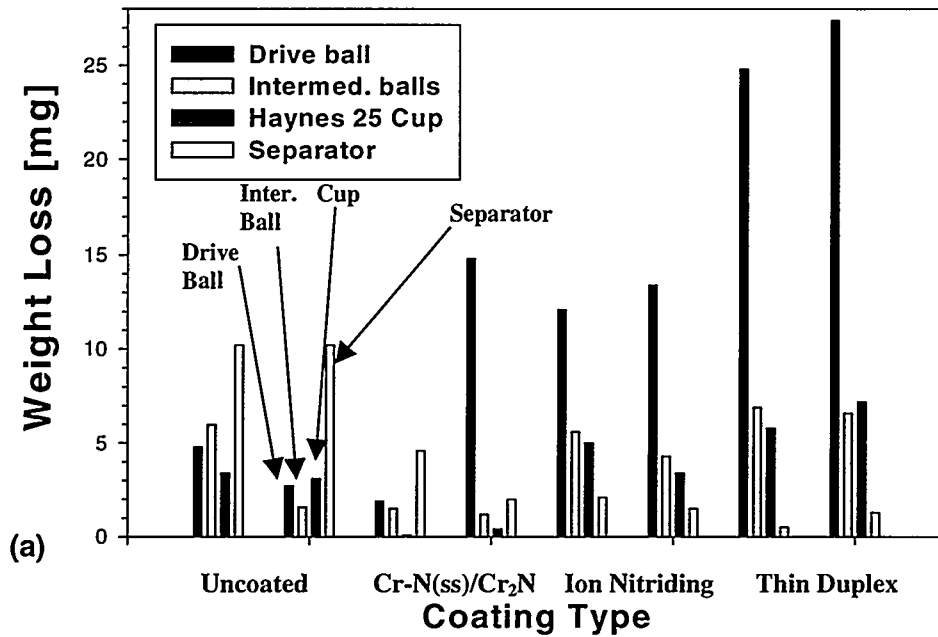


Figure 4. Summary of results from the 4-ball wear testing: (a) plot of weight loss for the uncoated and coated drive ball, intermediate ball (total of three), cup, and separator test specimens with two tests for the uncoated, Cr-N(ss)/Cr₂N coated, ion nitride, and thin duplex coated coupons, (b) post-test SEM of the surface of the Cr-N(ss)/Cr₂N coated cup, and (c) post-test SEM of the surface of the ion nitrided cup.

The VHN and scratch adhesion values for the duplex coatings were within the range of values previously measured for the Cr-N(ss)/Cr₂N coatings deposited on bare Haynes 25 (Table 1). The rough surface of the duplex coated coupons limited the accurate measurement of a critical load using the nano-scratch method. As observed for the ion nitride layer, coating damage was not observed in the scratch at the maximum load. This indicates that the duplex coatings are adherent and damage resistant. Nano-indentation hardness/modulus values for the thick duplex coating were higher than the ion nitrided surface and lower than uncoated Haynes 25 (Table 1). The deposition of the Cr-N(ss)/Cr₂N coatings on the compliant, iron-rich surface layer resulted in a coating with a lower nano-indentation hardness value for the duplex coatings than measured for the Cr-N(ss)/Cr₂N coatings deposited on bare Haynes 25. The duplex coating essentially consists of a hard nitride layer on Haynes 25 with a 1 µm thick iron-rich ductile layer on the nitride surface, and an outer dual-layer Cr-N(ss)/Cr₂N overcoating. The nano-indentation hardnesses are a nominal measure of the composite hardness of these layers. Since the nominal modulus/hardness values for the thick duplex coated substrate are lower than Haynes 25, and since this coating exhibits high critical load values, the duplex coatings are viable candidates. The scratch adhesion values

for the low-pressure nitrided, duplex coating are high than the thin dual layer Cr-N(ss)/Cr₂N coating in Table 1. Nano-indentation and VHN measurements in Table 1 indicate that the hardness of the low-pressure duplex coated surface is a close match to Haynes 25. However, the thin diffusion zone and coating thickness for the low-pressure duplex coating may be too thin to provide the desired wear protection.

B. Results of 4-ball Wear Testing

The thin Cr₂N/Cr-N(ss) coating, ion nitriding, and thin duplex coating were used for 4-ball wear testing [3]. Although the thick four-layer Cr-N(ss)/Cr₂N and thick duplex coatings also exhibited attractive properties, thin coatings are generally preferred for bearing applications. The wear of the cups was determined by weight change and pre- and post-test profilometry of the raceway (Taylor/Hobson Taly-surf profilometer). The weight change in Figure 4a and maximum wear depth in Table 3 for the uncoated coupons were fairly small in magnitude. The wear of the uncoated cup raceway was localized in one region of the raceway. The wear of the uncoated Haynes 25 drive ball was localized in a wear track due to high stress, ball-to-ball contact with the Stellite 3 intermediate balls (Table 3).

B1. Thin dual-layer Cr-N(ss)/Cr₂N coating

Table 3. Profilometry data for 4-ball wear test.

Wear Specimen	Number of Measurements	Surface Roughness, R_a [\AA]		Maximum Wear Depth [μm]
		Pre-test	Post-Test	
Uncoated Base-line Tests				
Cup - Test #1	1 - 4	250 - 1270	1600 - 4270	0.86 to 2.59
Drive Ball - Test #1	1	130	8740	26.1
Cup - Test #2	1 - 4	250 - 1270	1220 - 1350	0.64 - 1.24
Drive Ball - Test #2	1	130	10080	29.9
Thin Cr-N(ss)/Cr₂N Coating Tests				
Cup - Test #3	1 - 4	1350 - 1500	1450 - 1520	0.48 - 1.24
Drive Ball - Test #3	1	1350	8360	13.5
Cup - Test #4	1 - 4	1600-1980	1570 - 1960	0.41 - 1.14
Drive Ball - Test #4	1	1350	49,000	51.7
Intermediate Ball - Test #4	1	890	230	N/A
Ion Nitriding Surface Modification Tests				
Cup - Test #5	1 - 4	3020 - 4240	860 - 1630	1.19 - 1.45
Drive Ball - Test #5	1	2820	33,760	36.0
Intermediate Ball - Test #5	1	3660	840	N/A
Cup - Test #6	1 - 4	3050 - 8700	1520 - 2160	1.85 - 2.08
Drive Ball - Test #6	1	3250	33,530	24.8
Thin Duplex Coating: Ion Nitriding + Cr-N(ss)/Cr₂N Coating Tests				
Cup - Test #7	1 - 4	3610 - 3680	1270 - 1600	0.71 - 1.35
Drive Ball - Test #7	1	4140	42,880	35.3
Intermediate Ball - Test #7	1	1270	1070	N/A
Cup - Test #8	1	3380 - 4620	1240 - 1680	0.08 - 0.23
Drive Ball - Test #8	1	4140	45,420	36.9

The weight loss in Figure 4a for the Haynes 25 cup, Stellite 3 intermediate balls, and separator coated with a thin dual-layer Cr-N(ss)/Cr₂N coating were more than a factor of two less than the uncoated samples. The maximum wear depth for the Cr-N(ss)/Cr₂N coated cup in Table 3 (1.25 μm) was more than a factor of two less than the maximum wear depth of the uncoated cup (2.59 μm). Metallographic and SEM examinations indicated that the coating in the cup region was intact and undamaged over 99% of the cup surface, and small damage regions (less than 20 μm in diameter) such as that shown in Figure 4b were rarely observed. The pre- and post-test surface roughness for the Cr-N(ss)/Cr₂N coated cups and intermediate balls were identical in Table 3, which is further evidence that the coating was adherent. SEM and metallographic examinations confirmed that the coating was intact on 99% of the surface of the Stellite 3 intermediate balls. The weight loss and wear depth for one Cr-N(ss)/Cr₂N coated drive ball was much higher than the uncoated coupon. Low weight loss and wear depths were observed for the other Cr-N(ss)/Cr₂N coated Haynes 25 drive ball. Metallography and SEM of the worn Haynes 25 drive ball indicate that coating fracture and coating debris had resulted in significant wear damage in the wear track region of the drive ball. The failure of the thin Cr-N(ss)/Cr₂N coating in the region of ball-to-ball contact produced abrasive debris that increased the wear damage. These results indicate that the thin dual-layer Cr-N(ss)/Cr₂N coating cannot endure the high stress, ball-to-ball (point) contact loading at the drive-ball region. The harder Stellite 3 balls (Table 2) are subject to

less deformation from the ball-to-ball contact, and the thin dual-layer Cr-N(ss)/Cr₂N coating has remained adherent to provide excellent wear protection. These results show that the Cr-N(ss)/Cr₂N coating was tightly adherent on the Stellite 3 intermediate balls and Haynes 25 cup to result in a significant decrease in wear rate.

B2. Ion Nitriding

The ion nitrided Stellite 3 balls, Haynes 25 cup, and separator were observed to have a weight loss comparable to the uncoated samples in Figure 4a [3]. The maximum wear of the ion nitrided cup (2.08 μm) was slightly less than the uncoated cup (2.59 μm), see Table 3. A significant decrease in the surface roughness of the ion nitrided cup and intermediate ball surface was observed in Table 3 after the wear test. The wear of surface asperities on the as-received surface likely produced the larger weight losses observed for the ion nitrided Haynes 25 cup and Stellite 3 intermediate balls. Post-test SEM and metallographic examinations of the Haynes 25 cup and Stellite 3 intermediate balls in Figure 4c show the nitride layer was adherent with worn asperities. The pre-test and post-test thicknesses of the nitride layer were comparable for the Haynes 25 cup and Stellite 3 intermediate ball coupons, which indicates that the general wear of the nitride layer was slight. A uniform nitride layer was not deposited on the raceway of the Haynes 25 cup, and a region about 0.22 cm wide or about 1/3 of the 0.66 cm radius of the cup was observed to have no nitride layer. Improvements in the ion nitriding processing conditions (total pressure, nitrogen partial pressure, and plasma distribution) are needed to produce

Table 4. Summary of Results for pin-on-disc wear testing performed at ACT.

Test Number	Pin Coating / Disc Coating	Start Friction Coefficient	Maximum Friction Coefficient	Start Torque [kg-cm]	Maximum Torque [kg-cm]	Run Time [Minutes]
1	Uncoated/Uncoated	0.388	0.495	2.89	4.35	12
2	CrN/CrN	0.256	0.402	3.47	7.55	30
3	CrN/CrN	0.274	0.420	4.06	4.93	6
4	W/W	0.327	0.455	5.33	7.27	30
5	W/W	0.072	0.293	1.44	4.95	0.7
6	W/CrN	0.272	0.477	4.26	7.61	4
7	W/CrN	0.329	0.475	5.22	7.55	0.3
8	CrN/W	0.109	0.514	5.53	7.29	0.3
9	CrN/W	0.146	0.219	2.31	2.89	14

- Notes:
1. CrN = 2.5 μm thick chromium-nitride coating with a 3:2 ratio of Cr-N(ss) to Cr₂N layers.
 2. W = 9 μm thick tungsten coating.
 3. The pin was Stellite 3, the disc was Haynes 25.

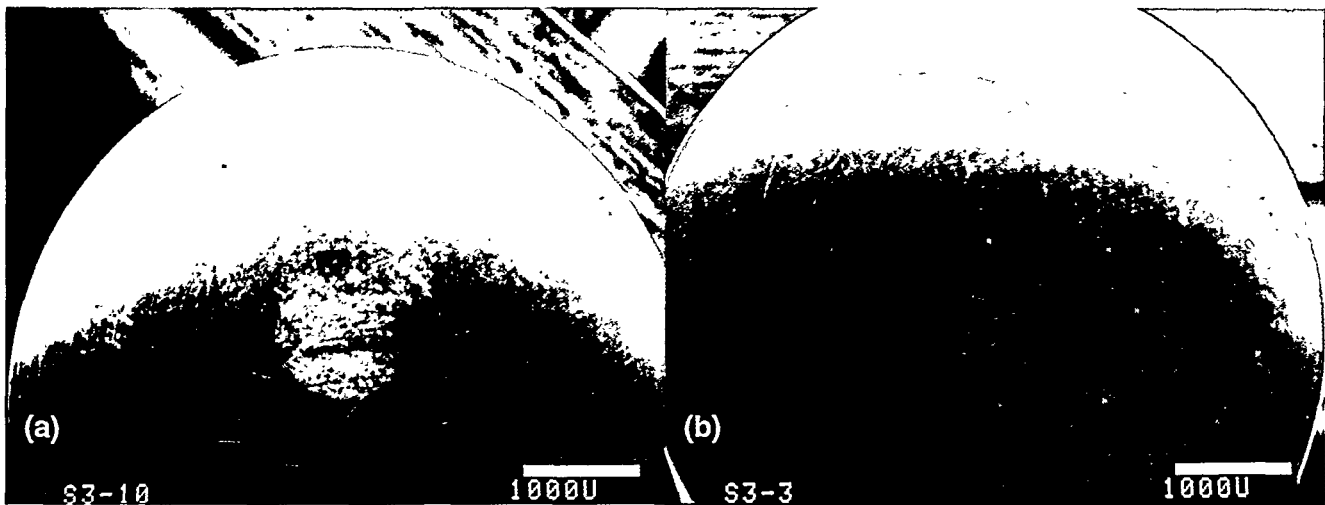


Figure 5. Post-test SEM examinations of the tip of Stellite 3 pin after pin-on-disc testing: (a) uncoated pin with adhesively transferred wear debris, and (b) Cr-N(ss)/Cr₂N coated pin showing little damage (Test #3 in Table 4).

an uniform nitride layer thickness in the cup raceway. The weight losses (Figure 4a) and wear depths (Table 3) for the ion nitrided Haynes 25 drive ball were larger than the uncoated drive ball. Metallographic and SEM examinations of the wear track on the Haynes 25 drive ball indicate that the ion nitride layer was generally adherent, but localized regions of nitride layer failure have produced wear debris that result in a higher wear rate. Although only limited damage was observed on the nitride layer for the Haynes 25 drive ball, these results indicate that the nitride layer was not resistant to the high-stress, ball-to-ball contact loading. The high stress, ball-to-ball contact loading did not produce failure or damage of the ion nitride layer on the Stellite 3 intermediate balls, which indicates the harder Stellite 3 substrate may provide the needed support for the nitride layer. The excellent adherence on the ion nitride layer on the Haynes 25 cup and Stellite 3 indicates that this process may be viable with improvements in the processing conditions.

B3. Duplex Coatings (Ion Nitriding + Cr-N(ss)/Cr₂N Coatings)

The duplex coated Stellite 3 balls, Haynes 25 cup, and uncoated separator exhibited weight changes in Figure 4a that were comparable to or only a factor of two higher than the uncoated samples. The duplex coated cup had a maximum wear depth (1.27 μm) in Table 3 that was more than a factor of two less than the uncoated cup (2.59 μm). The surface roughness of the thin duplex coated Haynes 25 cup and Stellite 3 intermediate balls was significantly less after testing, as previously observed for the ion nitrided coupons in Table 3. The surface asperities

on the rough as-deposited surface had been fractured off during the wear test for a decrease in surface roughness with higher weight losses. Post-test SEM and metallographic examinations of the duplex coated Haynes 25 cup and Stellite 3 intermediate balls show that the outer Cr-N(ss)/Cr₂N coating was fairly intact. The post-test thickness of the outer Cr-N(ss)/Cr₂N layer on the duplex coated surfaces were much thinner than the post-test thickness of the Cr-N(ss)/Cr₂N coatings deposited on bare Haynes 25. The fracturing of fine surface asperities during the 4-ball wear testing of the duplex coated coupons produces hard debris that results in a higher wear rate for the thin duplex coated cups. The duplex coated Haynes 25 drive balls experienced a significantly higher weight loss (Figure 4a) and wear depth (Table 3) than observed for the uncoated drive balls. The failure of the Cr-N(ss)/Cr₂N coating produced hard debris that resulted in more significant wear of the duplex coating than observed for the ion nitrided Haynes 25 drive ball. The duplex coating cannot survive the high-stress, point-to-point contact loading when deposited on Haynes 25. The thin duplex coating has survived the high-stress, point-to-point contact loading when deposited on the Stellite 3 intermediate balls, which indicates that the harder Stellite 3 substrate supports the thin duplex coating. Improvements in the processing conditions could improve the performance of the duplex coatings.

C. Pin-on-Disc Wear Testing

The pin-on-disc wear tests were performed to evaluate the general wear resistance of Cr-N(ss)/Cr₂N coatings and a less-hard, thick tungsten coating that does not have multiple-layers, see Table 1. The summary of test results shows in Table 4 that the uncoated base-line test was terminated early because of high torque or friction values. SEM examination shows in Figure 5a that the uncoated Stellite 3 tip has been worn flat and Haynes 25 wear debris has been adhesively transferred from the pin to the disc. Deep grooves and a high surface roughness were observed for the uncoated Haynes 25 disc.

C1. Thin dual-layer Cr-N(ss)/Cr₂N coating

The longest run times were observed for the self-mated Cr-N(ss)/Cr₂N coated specimens (Tests #2 and #3 in Table 4). Lower friction values and slightly higher torque values were observed for the self-mated Cr-N(ss)/Cr₂N coated coupons in comparison to the uncoated coupons. The high-stress, point contact resulted in the Cr-N(ss)/Cr₂N coating being worn off the pin in Figure 5b. The maximum diameter of the worn tip of the Cr-N(ss)/Cr₂N coated pin (930 μm) was much less than the uncoated pin (1050 μm). The worn tip of the Cr-N(ss)/Cr₂N coated pin was much smoother than the uncoated pin, and no transfer of wear debris was detected. Significantly less wear and roughening was observed on the Cr-N(ss)/Cr₂N coated Haynes 25 disc compared to the uncoated Haynes 25 disc. The excellent durability and wear resistance observed for the self-mated Cr-N(ss)/Cr₂N pin-on-disc test indicates that this combination is a good wear couple, which is consistent with the excellent results observed in the 4-ball wear test.

C2. Tungsten and Mixed Couples

Although the friction coefficient and torque observed for the self-mated tungsten coating tests were comparable to the self-mated Cr-N(ss)/Cr₂N coating tests in Table 4, the run time was very short for one test. A significantly greater amount of coating wear damage was observed in post-test SEM examination of the tungsten coated pin and disc coupons. The mixed couple tests consisting of tungsten coated pins mated with Cr-N(ss)/Cr₂N coated discs (Test #6 and #7 in Table 4) and Cr-N(ss)/Cr₂N coated pin mated with tungsten coated discs (Tests #8 and #9 in Table 4) had torque and friction values comparable to the self-mated Cr-N(ss)/Cr₂N coated tests. The significantly shorter run times and greater amount of damage observed for the mixed couple tests indicates that the wear resistance of the self-mated couples was generally better. The best wear performance in the pin-on-disc test was observed for the self-mated Cr-N(ss)/Cr₂N coated specimens.

Summary

High interfacial stresses and coating failure are expected when a hard coating is used to cover a more-compliant substrate in applications involving high stress wear contact [4,5]. Assuming small differences in stiffness (or modulus) between the coating and substrate are required for a wear resistant coating to be used in such applications, four approaches have been taken to develop wear resistant coatings for cobalt-base alloys. Hardness, scratch adhesion, and nano-indentation testing results in Table 1 have been used to identify the most promising candidates for cobalt-base alloys that are based on these four approaches: (1) use of a thin coating with hard Cr₂N and less-stiff Cr-N(ss) layers, (2) the use of a thick, four-layered coating with a 4 μm inner layer of Cr-N(ss) / 1 μm layer of Cr₂N / 4 μm layer of Cr-N(ss) / 1 μm outer layer of Cr₂N, (3) a duplex approach of ion nitriding to harden the subsurface followed by application of a dual-layered Cr₂N/Cr-N(ss) coating, and (4) use of ion nitriding alone. The low scratch adhesion values and high modulus/hardness values indicate that ZrN, TiN, and plasma carburized coatings represent less desirable approaches.

Based on weight change (Figure 4), profilometry measurements (Table 3), and metallographic and SEM examinations after 4-ball wear testing, the thin Cr₂N/Cr-N(ss) coated coupons exhibited a significantly

lower wear rate than the uncoated Haynes 25 coupons. More importantly, the thin Cr₂N/Cr-N(ss) coatings were adherent on the Stellite 3 intermediate balls and Haynes 25 cups, and prevented the wear of the cobalt-base substrate. Based on these results, the thin Cr₂N/Cr-N(ss) coating was the best coating candidate, and use of this coating could result in a reduced wear rate and less cobalt wear debris. The ion nitrided coupons exhibited slightly higher wear than the thin Cr₂N/Cr-N(ss) coated coupons, while the wear of the thin duplex coated coupons was the highest. The nitride layer was adherent and protected the Haynes 25 substrate. Modification of the ion nitriding conditions or surface lapping after nitriding are approaches that may improve the wear resistance of the ion nitriding and duplex coatings.

The pin-on-disc testing was performed to evaluate the wear of self-mated coated surfaces. Based on friction values, torque values, run time, and post-test SEM examinations, the self-mated Cr₂N/Cr-N(ss) coated pin and disks exhibited better wear resistance than the uncoated specimens, with lower friction values, longer run times and less surface damage observed in SEM (Table 4 and Figure 5). The wear of the self-mated, Cr₂N/Cr-N(ss) coated specimens was better than the self-mated tungsten, or mixed couple specimens. The excellent wear resistance of the self-mated Cr₂N/Cr-N(ss) coated substrates agrees with the good results observed in 4-ball wear testing.

Acknowledgement

This work was performed under USDOE Contracts DE-AC11-93PN38195 and DE-AC11-98PN38206. The technical assistance and contributions of J. L. Hollenbeck, W.L. Wilson, and R.R. Koch are appreciated. I am also grateful for the support of various Bettis Atomic Power Laboratory personnel in completing this work (F.W. Page, S.A. Vazquez, G.A. Hoffman, T.A. Dobrich, D.M. Gasparovic, A. Stinson, and D.L. Ward).

References

- [1] *Friction, Lubrication, and Wear Technology*, Materials Handbook Vol. 18, ASM-I, Materials Park, OH, p.758 (1992).
- [2] E.K. Ohriner, T. Wada, E.P. Whelan, and H. Ocken, *Met. Trans.*, 22A, 983-991 (1991).
- [3] B.V. Cockeram, *Surface and Coatings Technology*, in press. Available as B-T-3237 from DOE/OSTI (Oak Ridge, TN 1999).
- [4] L. Zheng and S. Ramalingam, *J. Vac. Sci. Technol. A*, 13, 2390-2398 (1995).
- [5] L. Zheng and S. Ramalingam, *Surface and Coatings Technology*, 81, 52-71 (1996).
- [6] *The Rolltact Test Machine*, Industrial Tectonics Report No.106, Industrial Tectonics, Inc., Compton, CA (1988).
- [7] T.Y. Tsui, G.M. Pharr, W.C. Oliver, Y.W. Chung, E.C. Cutiongco, C.S. Bhatia, R.L. White, R.L. Rhoades, and S.M. Gorbakhin, *MRS Res. Soc. Symp. Proc.*, 356, 767-772 (1995).
- [8] W.C. Oliver and G.M. Pharr, *J. Mater. Res.*, 7, 1564-1583 (1992).
- [9] A.J. Perry, J. Valli, and P.A. Steinmann, *Surface and Coatings Technology*, 36, 559-575 (1988).
- [10] A.H. Deutchman, R.J. Partyka, and C. Lewis, *Proceedings of 2nd International Conference on Ion Nitriding/Ion Carburizing*, pp. 29-36, ASM International, Materials Park, OH (1990).
- [11] P.H. Nowill, *Proceedings of 2nd International Conference on Ion Nitriding/Ion Carburizing*, pp. 175-176, ASM International, Materials Park, OH (1990).